ORIGINAL ARTICLE

Preparation and evaluation of castalin (hydrolysable tannin)-loaded poly (lactic-co-glycolic acid) nanoparticles and exploring its anticancer potential

J. Praveen Kumar[1]*, P. Geetha[2]

[1]Research Scholar, Vels Institute of Science and Technology Advanced Studies, Chennai, Tamil Nadu, India, [2]Department of Pharmaceutics, Vels Institute of Science and Technology Advanced Studies, Chennai, Tamil Nadu, India

Abstract

Aim: Over the past few decades, nanoparticles (NPs) have gained immeasurable interest in the field of drug delivery. Various NP formulations have been disseminated in drug development in an attempt to increase efficiency, safety, and tolerability of incorporated drugs. In this context, NP formulations that increase solubility, control release, and/or affect the *in vivo* disposition of drugs were developed to improve the pharmacokinetic and pharmacodynamic properties of encapsulated drugs. Among the potent anticancer agents, castalin has been found to be very efficacious against many different types of cancer cells. Our present work investigated the efficiency of encapsulation of castalin in poly(lactic-co-glycolic acid) (PLGA) NPs using solid/oil/water emulsion solvent evaporation method. **Materials and Methods:** The NPs were formulated and then characterized for percent yield, encapsulation efficiency, surface morphology, particle size, drug distribution studies, drug polymer interaction studies, and *in vitro* drug release profiles. The objective of this work is to prepare and evaluate PLGA NPs of castalin, an anticancer agent loaded by solvent displacement method using stabilizer (polyvinyl alcohol). **Results and Discussion:** The prepared NPs were characterized by Fourier transmission infrared (FT-IR), differential scanning calorimetry (DSC), drug loading, entrapment efficiency, particle size, and surface morphology by atomic force microscopy (AFM), X-ray diffraction, and *in vitro* studies. FT-IR and DSC studies indicated that there was no interaction between the drug and polymer. The morphological studies performed by AFM showed uniform and spherical-shaped discrete particles without aggregation and smooth in surface morphology with a nano size range of 144 nm. **Conclusion:** In this context, the huge number of reports on PLGA NPs used as drug delivery systems in cancer treatment highlights the potential of PLGA NPs as drug carriers for cancer therapeutics and encourages further translational research.

Key words: Nanoparticles, poly(lactic-co-glycolic acid), castalin, cancer, sustained release, target delivery

INTRODUCTION

The field of nanomedicine, which refers to the application of nanotechnology in medicine, offers valuable tools for the diagnosis and treatment of diseases. In this regard, a wide range of submicron materials has been designed and engineered, especially for defeating cancer. Its applications expedite the development of contrast agents, therapeutics, drug delivery vehicles, and theranostics. Nanoparticles (NPs) for drug delivery applications have been composed of biodegradable and biocompatible polymers based on natural and/or synthetic materials. Synthetic polymers can be produced with high purities in a precise and well-controlled production process, as compared to natural products.[1-5]

NPs are small particles that range in size from 10 nm to 1000 nm.[1] They contain nanomolecular materials in which active ingredients are dissolved, entrapped, and/or encapsulated. At present, NPs can be found in hundreds of different consumer products ranging from sunscreen and air conditioners to processed food supplies.[2] Over the past few

Address for correspondence:
J. Praveen Kumar, Research Scholar, Vels Institute of Science and Technology Advanced Studies, Chennai, Tamil Nadu, India. Mobile: +91-9966876409.
E-mail: jaldupraveen@gmail.com

Received: 28-06-2021
Revised: 21-08-2021
Accepted: 28-08-2021

decades, NPs have gained recognition in the medical field as an effective means of drug delivery and therapy.[3]

One extensively investigated polymer is poly(lactic-co-glycolic acid) (PLGA), synthetic thermoplastic aliphatic biocompatible polyester. There are specific formulations based on PLGA and its related homo polymers; poly(lactic acid) (PLA) and poly(glycolic acid) (PGA), which have been approved by the US Food and Drug Administration (FDA) for medical applications.[4] PLGA NPs have also proved their potential as drug delivery systems for many therapeutic agents (e.g. chemotherapy, antibiotics, antiseptic, anti-inflammatory and antioxidant drugs, and proteins) and can be favorable for tumor and/or DNA.[6-11]

At present, there are many types of polymers available for polymer-based NP formulation. Examples of common polymers employed in NP formulation are PLA, PGA, and PLGA.[4] Like many NP delivery systems, polymer-based NP formulation can act to offset drug release by desorption of bound drug from particle surfaces, erosion of the polymer membrane, and/or drug diffusion.[4] The three aforementioned stages at which polymer NPs can release active pharmaceutical agents make them an ideal choice in attempting to formulate a new and novel drug delivery systems that could act to modify or control drug release and offset the occurrence of drug-related adverse events.

MATERIALS AND METHODS

Castalin PLGA (lactide/glycolide = 50:50, Resomer® 503H) was purchased from Boehringer Ingelheim Pharma Gmbh and Co., Germany. Tocopheryl polyethylene glycol succinate (TPGS) and acetone were obtained from Sigma-Aldrich, India. HepG2 cell line was obtained from Amla Cancer Research Institute, India.

Preparation of Castalin NPs

The ellagitannins are a diverse class of hydrolyzable tannins, a type of polyphenol formed primarily from the oxidative linkage of galloyl groups in 1,2,3,4,6-pentagalloyl glucose. Ellagitannins differ from gallotannins, in that their galloyl groups are linked through C-C bonds, whereas the galloyl groups in gallotannins are linked by depside bonds. It can be found in oak wood and *Melaleuca quinquenervia* is botanical name and family Myrtaceae.

Castalin-loaded PLGA NPs were prepared by nanoprecipitation technique. Briefly, 100 mg of PLGA was dissolved in 1 mL acetone and then added drop wise to 10 mL of TPGS solution (0.3% w/v) with continuous stirring. Castalin 10 mg was dissolved into 10 ml of water. Organic phase obtained with the addition of PLGA and TPGS solution in acetone was added dropwise to aqueous phase of castalin solution on stirring. Acetone was allowed to evaporate by continuous magnetic stirring for 4 h. Castalin-loaded PLGA NPs were then recovered from the nanodispersion by centrifugation at 15,000 g force for 35 min at 4°C. Then, precipitated PLGA NPs were suspended in mannitol solution (5% w/v) and lyophilized for 72 h.

Experimental Design

Preliminary experiments indicated that the variables, such as drug polymer ratio, aqueous to organic phase ratio, and stirring time during preparation, were the main factors that affected the particle size, size distribution, and process yield and entrapment efficiency (EE) of the castalin NPs. Thus, a central composite rotatable design–response surface methodology (CCRD–RSM) was used to systemically investigate the influence of these three critical formulation variables on particle size, % yield, and % EE of the prepared NPs. The details of the design are listed in Table 1. For each factor, the experimental range was selected on the basis of the results of preliminary experiments and the feasibility of preparing the NPs at the extreme values. The value range of the variables was drug polymer ratio (X1) of 1:1–1:7, ratio of aqueous to organic phase (X2) of 1:1–1:5, and stirring time (X3) of 15–45 min. A total of 20 tests were conducted. All the formulations in these experiments were prepared in duplicate.

Characterization of the NPs

Particle size, polydispersibility index, and zeta potential

Particle size analysis was performed by dynamic light scattering (DLS) with a Malvern Zetasizer 3000 HSA (Malvern Instruments, UK). DLS yields the mean diameter and the polydispersity index (PI) which is a measure of the width of the size distribution. The mean diameter and PI values were obtained at an angle of 90° in 10 mm diameter cells at 25°C. Before the measurements, all samples were diluted with double-distilled water to produce a suitable scattering intensity.

Zeta Potential

The zeta potential, reflecting the electric charge on the particle surface and indicating the physical stability of colloidal systems, was measured by determining the electrophoretic

Table 1: Independent variables and their corresponding levels of NP preparation

Independent variables	Levels		
	-1	0	+1
Drug/polymer ratio	1:1	1:4	1:7
Aqueous to organic phase ratio	1:1	1:3	1:5
Stirring time	15	1:30	45

NP: Nanoparticle

mobility using the Malvern Zetasizer 3000 HSA (Malvern Instruments, UK). The sample was measured in double-distilled water and adjusted to a conductivity of 50 IS/cm with sodium chloride solution (0.9% w/v). The pH was in the range of 5.5–7.5 and the applied field strength was 20 V/cm.

Scanning Electron Microscopy (SEM) Measurement

The samples for SEM were mounted on metal stubs, and the surface and surface morphology of the particles were examined by a Hitachi S4800 Field Emission SEM (Hitachi, Gaithersburg, MD, USA). The analytical parameters included an accelerating voltage of 10 KeV, a working distance of 13.5 mm, and a vacuum of 40 Pascals.

Differential Scanning Calorimetry (DSC) Analysis

A DSC (Shimadzu DSC-60, Columbia, MD, USA) was used to analyze pure castalin, PLGA, and physical mixture and castalin NPs. The sample to be analyzed (3–5 mg) by DSC was crimped non-hermetically in an aluminum pan and heated from room temperature (23°C) to 300°C at a rate of 10°C/min under nitrogen purge.

Fourier-Transmission Infrared (FTIR) Spectroscopy analysis

FTIR analyses of castalin, PLGA, physical mixture, and castalin NPs were carried out using IR Prestige-21 (Shimadzu, Columbia, MD, USA). The sample was placed in direct contact with ATR crystal ensuring good contact. All the spectra were recorded as a mean of 20 scans, with a resolution of 4 cm^{-1} and in the range of 800–4000 cm^{-1}.

Chromatographic Conditions

The concentration of castalin was detected by high-performance liquid chromatography (HPLC) system using a C18 Luna column 5 µm particle size, 25 cm × 3.00 mm I.D. (Phenomenex, Torrance, CA, USA). A mobile phase composed by water-formic acid (99.5:0.5, v/v) (solvent A) and acetonitrile (solvent B) was used. The flow rate was 0.5 ml/min. The injection volume was 10 µL and the wavelength was set at 246 nm.

Determination of Drug EE and Process Yield

The nanoformulations were centrifuged and the supernatant containing free drug was collected which was further analyzed by HPLC at 246 nm. This gives the amount of drug that is unentrapped in the NPs. Amount of drug found in the supernatant was subtracted from the total amount of drug added to the formulation which gives the amount of drug entrapped in the NPs. The formulations were evaluated for EE by the following formula:

$$EE=\frac{\text{Mass of drug in nanopartilce}}{\text{Mass of drug used in the formulation}}\times 100\%$$

Process Yield

The yield of NPs was calculated using the following equation:

$$\text{Yield}=\frac{\text{Mass of nanoparticles recovered}}{\text{Mass of polymer+drug+excipients}}\times 100$$

In vitro Release Study

One hundred milliliters of phosphate buffer, pH adjusted to 7.4 were poured into a well-closed glass vessel as the dissolution medium for the *in vitro* release test. Castalin NP (5 ml) was transferred to a dialysis bag (molecular weight cutoff 5000–10,000) and then the dialysis bag was placed in the glass vessel. The vessels were placed in an incubator shaker and shaken horizontally (Incubator Shaker ZHWY-200B, Shanghai Zhicheng Analysis Instrument Company, China) at 37°C and 100 strokes per min. The sample (1 ml) was withdrawn from the system at predetermined time intervals and filtered through a 0.45 µm hydrophilic filter membrane. The drug content was measured by the HPLC method described above. The diffusion profile of pure drug suspension through a dialysis bag was examined as control. The pure drug suspension was prepared by dispersing 1 ml castalin solution (5 mg/ml) in 4 ml of double-distilled water. Each experiment was performed in triplicate.

Nitric Oxide (NO) Radical Scavenging Assay

Sodium nitroprusside in aqueous solution at physiological pH spontaneously generates NO which interacts with oxygen to produce nitrite ions that can be measured using Griess reagent at 546 nm spectrophotometrically.

Nitric oxide scavenging assay is carried out the scavenging activity of the plant extracts against nitric oxide radical.[6] In brief, 200 µl of 10 mM sodium nitroprusside and 200 µl of test solution/reference standard of various concentrations are incubated at room temperature for 150 min. Add 500 µl Griess reagent and incubated for 10 min at room temperature. Measure the absorbance at 546 nm spectrophotometrically. Test substances are replaced by buffer solution for a control.

Cytotoxicity Studies using HepG2 Cell Line by MTT Assay

HepG2 cell line was obtained from Amla Cancer Research Institute, India. A total of 50,000 cells/well were taken and seeded in 96-well plates and incubated for 24 h at 37°C, 5% CO_2 incubator. Castalin and castalin NPs to be tested are added from 0 to 320 µg/ml concentration in RPMI without FBS and

are incubated for 24 h. One hundred microliters/well of the MTT (5 mg/10 ml of MTT in 1× PBS) were added to incubate the castalin and castalin NPs samples to the respective wells and incubated for 3–4 h. MTT reagent was discarded by pipetting without disturbing cells and 100 µl of DMSO was added rapidly to solubilize the formazan. Absorbance was measured at 590 nm. Inhibition calculation is made using the formula:

$$\% \text{ Inhibition} = 100 - \left(\frac{\text{OD of sample}}{\text{OD of control}}\right) \times 100$$

Storage Stability

The storage stability of optimized NPs was determined as follows. Briefly, an aliquot of 15 ml NPs suspension with 1 mg/ml drug concentration was placed into glass vials and stored at 4 and 25°C in the dark for 180 days, and the changes of particle size and zeta potential against storage time were investigated. Furthermore, drug EE against storage time were determined under 4°C. Before the measurement of particle size, zeta potential, and EE, the NPs powders were redispersed in distilled water with 1 mg/ml drug concentration by vortexing for 3 min. The particle sizes, zeta potential values, and EE of the NPs were determined by the method described above.

Data Analysis

The relationships between responses and formulation variables of all model formulations were treated by Design-Expert® software. Statistical analysis including stepwise linear regression and response surface analysis was conducted. The significant terms ($P < 0.05$) were chosen for final equations. Suitable models consisting of three components include linear, quadratic, and special cubic models. The best fitting mathematical model was selected based on the comparisons of several statistical parameters including the coefficient of variation (c.v.), the multiple correlation coefficient (R2), and the adjusted multiple correlation coefficient (adjusted R2) proved by Design-Expert software. Significance of differences was evaluated using Student's *t*-test and one-way ANOVA at the probability level of 0.05.

RESULTS AND DISCUSSION

The CCRD–RSM constitutes an alternative approach because it offers the possibility of investigating a high number of variables at different levels with only a limited number of experiments. The variables in Table 1 were chosen taking into account our preliminary experiments. Table 2 shows the experimental results concerning the tested variables on drug EE, process yield, and mean diameter of particle size. The three dependent values ranged from 83% to 98% by weight, 61% to 93% by weight, and 153 nm to 210 nm. A mathematical relationship between factors and parameters was generated by response surface regression analysis using Design-Expert® 7.0 software. The three-dimensional (3D) response surface graphs for the most statistical significant variables on the evaluated parameters are shown in Figures 1-4. The response surface diagrams showed that an increase in polymer concentration and aqueous to organic phase ratio increases the particle size and EE. Process yield of s decreases at a stage increasing both the polymer concentration and aqueous to organic phase ratio. The optimized variables showed a good fit to the second-order polynomial equation, with correlation coefficient (r) of 0.9677, 0.7574, and 0.7398, respectively. After model simplification with backward stepwise solution, the r value decreased slightly to 0.9387, 0.6454, and 0.5055, respectively. The lack of it was not significant at 95% confidence level. All the remaining parameters were significant at $P \leq 0.05$. It was observed that the best fitted model was the quadratic model, and the comparative values of R, SD, and % CV along with the regression equation generated for the selected responses are given in Table 3. The statistical analysis of the results generated the following polynomial equations:

The fitting results indicated that the optimized NPs with high EE, high yield, and small mean diameter were obtained at the drug polymer ratio of 1:1, aqueous to organic phase ratio of 1:5, and stirring time of 21 min, respectively. Table 4 shows that the experimental values of the two batches prepared within the optimum range were very close to the predicted values, with low percentage bias, suggesting that the optimized formulation was reliable and reasonable. Perturbation plots in Figures 5-7 reveal the impact of an independent factor on a particular response, with all various other aspects held consistent at a referral factor. A steep incline or curvature suggests sensitiveness of the response to a specific factor. Figure 5 shows that stirring time had one of the most crucial impacts on particle size followed by aqueous to organic phase ratio and drug polymer ratio. Figure 6 shows that stirring time had one of the most crucial impacts on EE followed by aqueous to organic phase ratio and drug polymer ratio. Figures 7-10 reveals that aqueous to organic phase ratio had the most crucial result on process yield followed by stirring time and drug polymer ratio.

DSC Analysis

DSC was performed to analyze the physical state of castalin within the PLGA NPs on the preparation. Thermogram of PLGA showed a sharp endothermic peak at 40–60°C [Figure 11]. The pure castalin shows a sharp endothermic peak that corresponds to melting point at 210–215°C. The representation of the weak peaks obtained corresponding to castalin in the DSC thermogram of the NPs suggests that the drug is well dispersed in the formulation.

Fourier-Transmission Infrared (FTIR) Spectroscopy Analysis

FTIR analysis is used to study the interactions between castalin, PLGA, physical mixture, and the drug-loaded NPs

Table 2: CCRD generated by Design-Expert 11® software along with the obtained response

Std.	Run	Factor 1 A: Drug polymer	Factor 2 B: Aqueous to or	Factor 3 C: Stirring time min	Response 1: Particle size nm	Response 2: EE %	Response 3: Process yield %
15	1	4	3	30	210	92	90
20	2	4	3	30	210	92	90
7	3	1	5	45	179	98	76
2	4	7	1	15	176	90	66
11	5	4	–0.363586	30	191	88	84
17	6	4	3	30	210	92	90
8	7	7	5	45	183	97	64
12	8	4	6.36359	30	165	94	93
16	9	4	3	30	210	92	90
18	10	4	3	30	210	92	90
5	11	1	1	45	186	94	70
13	12	4	1	4.77311	170	88	87
4	13	7	5	15	161	87	65
19	14	4	3	30	210	92	90
3	15	1	5	15	153	87	86
1	16	1	1	15	172	95	76
9	17	–1.04538	3	30	177	92	61
6	18	7	1	45	159	87	73
14	19	4	3	55.2269	189	90	90
10	20	9.04538	3	30	166	83	75

CCRD: Central composite rotatable design, entrapment efficiency, EE: Entrapment efficiency

Table 3: Reduced response models and statistical parameters obtained from ANOVA

Responses	Regression model	Adjusted R^2	Model *P*-value	%CV	Adequate precision
Particle size	PS=210.10-2.16A-4.45B+5.63C+4.37AB-4.38AC+6.37BC-14.28A^2-11.98B^2-11.45C^2	0.9387	0.0001	2.65	17.57
EE	EE%=91.10-2.06A+0.9585B+1.49C+1.37AB-0.3750AC+3.13BC	0.6454	0.0001	2.41	10.04
Process yield	Yield %=90.30-1.20A+1.55B-0.3628C-3.25AB+2.75AC-1.50BC-9.71A^2-2.46B^2-2.46C^2	0.5055	0.0001	3.12	24.05
Acceptance criteria		1	<0.05	<4	>10

EE: Entrapment efficiency

Table 4: Comparison of experimental and predicted values under optimal conditions for final formulation

Drug/polymer ratio	Aqueous to organic phase ratio	Stirring time (min)	Particle size (nm)	EE (%)	Process yield (%)
1:1	1:5	21.66			
Predicted			164	89.9	85.9
Experimental			164	89.0	85.0
Bias %			0	1.0	1.0
Acceptance criteria 6%					

Bias was calculated as (predicted value - experimental value)/predicted value ×100, EE: Entrapment efficiency

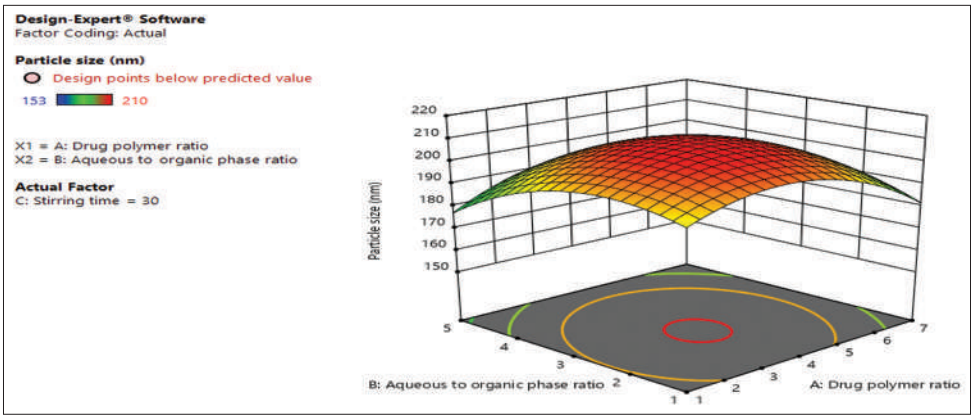

Figure 1: Three-dimensional (3D) response surface plots showing the effect of the variable on response. The effect of drug/polymer ratio and aqueous to organic phase ratio on particle size

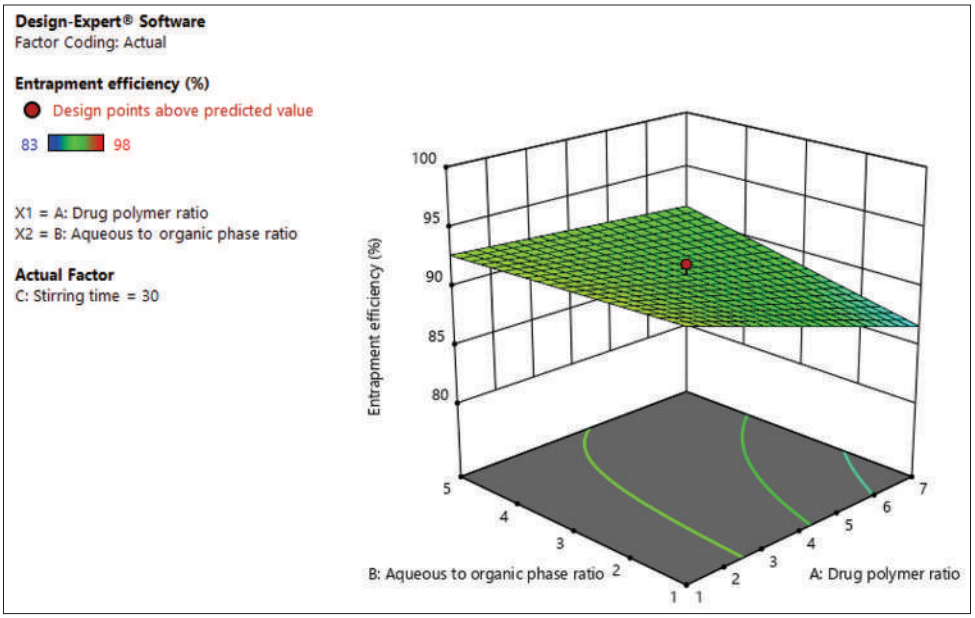

Figure 2: Three-dimensional (3D) response surface plots showing the effect of the variable on response. The effect of drug/polymer ratio and aqueous to organic phase ratio on entrapment efficiency

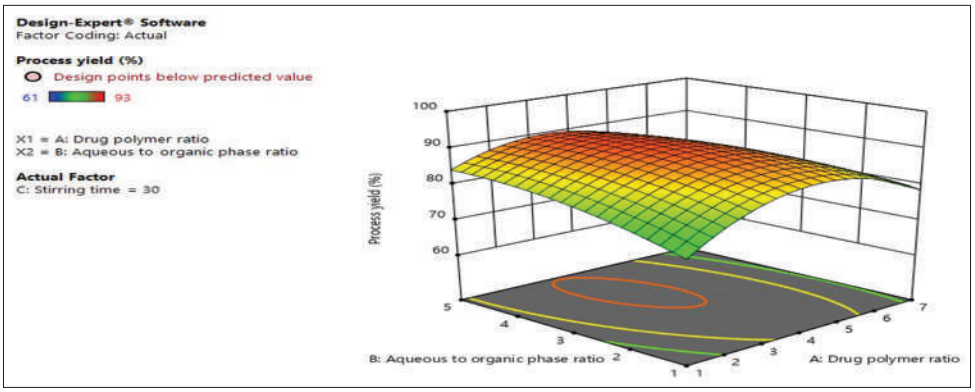

Figure 3: Three-dimensional (3D) response surface plots showing the effect of the variable on response. The effect of drug/polymer ratio and aqueous to organic phase ratio on process yield

and the spectrum obtained is presented in Figure 12. The IR of the mixture of drug sample and PLGA was found to be within the specified range. Hence, there is no interaction between the drug sample and PLGA and can be well used in the formulation. Castalin procured their entire characteristic peak in physical mixture. That is, significant peak 750–1580

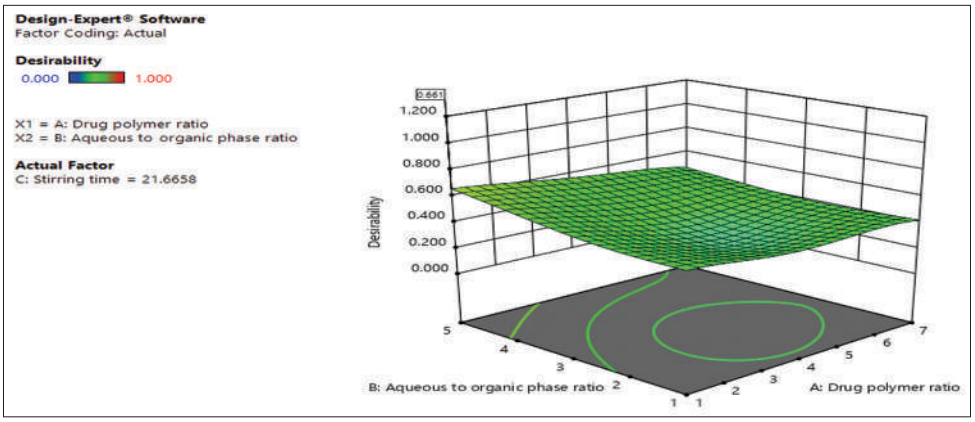

Figure 4: Three-dimensional (3D) response surface plots showing the desirability with a value of 0.66

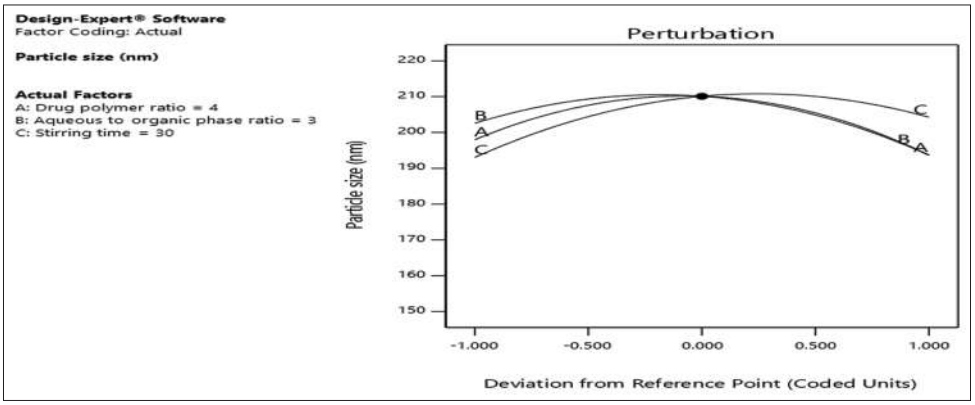

Figure 5: Perturbation plot showing the effect of each of the independent variables on particle size where A, B, and C are drug/polymer ratio, aqueous to organic phase ratio, and stirring time, respectively

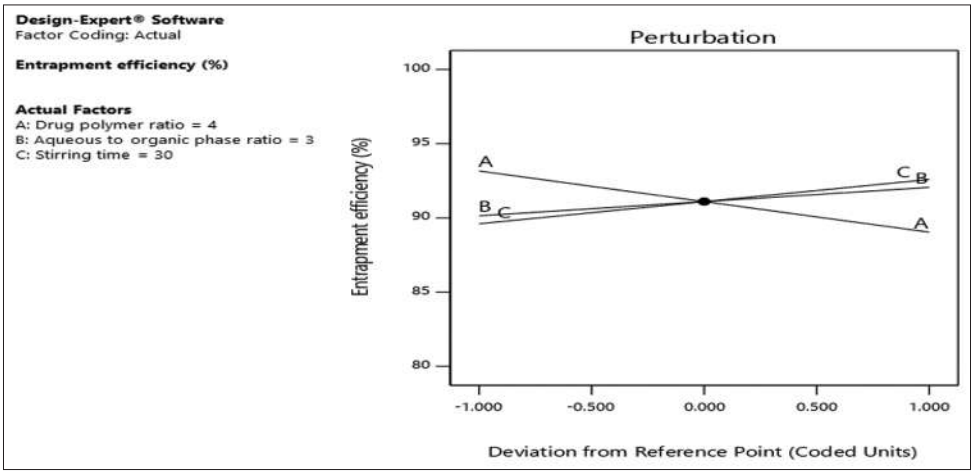

Figure 6: Perturbation plot showing the effect of each of the independent variables on entrapment efficiency where A, B, and C are drug/polymer ratio, aqueous to organic phase ratio, and stirring time, respectively

was retained in the physical mixture. Peak at 2890 and 3100 was prominent in castalin along with the physical mixture. In fingerprint region of castalin, the characteristic band at 850 and 1350–1580 was retained in the physical mixture. On the basis of FTIR spectra investigation, no chemical interaction was observed between castalin and PLGA.

In vitro Drug Release Study

The *in vitro* release behavior of castalin from the solution and NPs was studied for more than 180 h, as shown in Figure 13. As it was shown, drug release from the solution and the NPs occurred in a biphasic manner of burst release and sustained

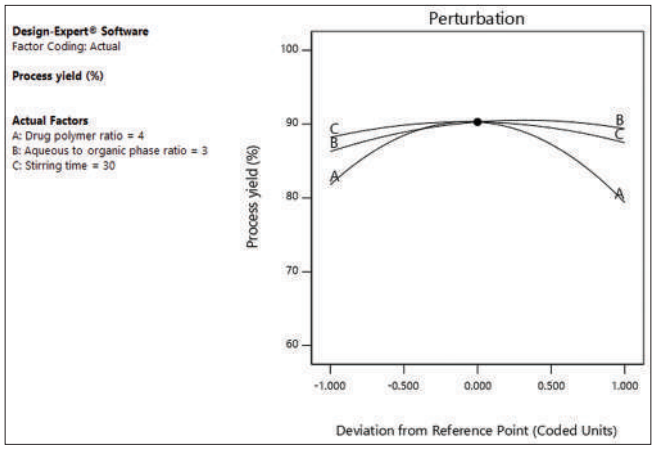

Figure 7: Perturbation plot showing the effect of each of the independent variables on process yield where A, B, and C are drug/polymer ratio, aqueous to organic phase ratio, and stirring time, respectively

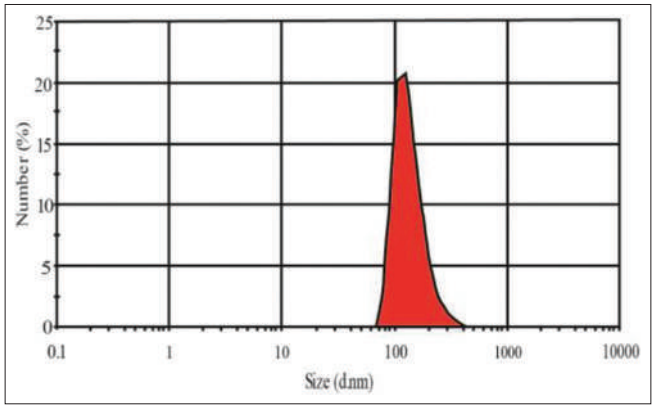

Figure 8: Particle size of optimized castalin nanoparticles

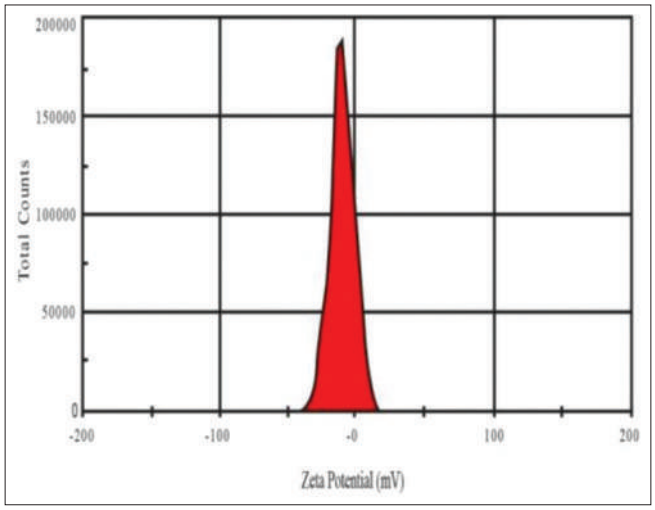

Figure 9: Zeta potential of optimized castalin nanoparticles

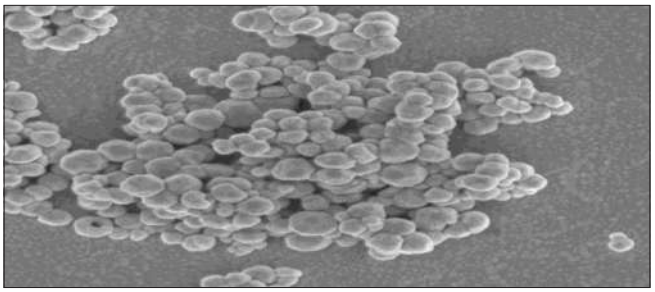

Figure 10: Scanning electron microscopy image of optimized castalin nanoparticles

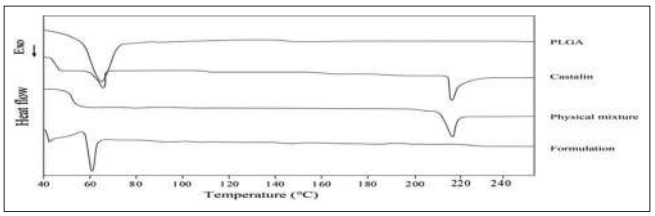

Figure 11: Differential scanning calorimetry of castalin, poly(lactic-co-glycolic acid), physical mixture, and nanoformulation

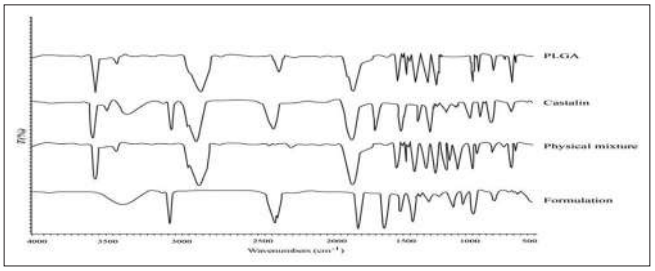

Figure 12: FTIR analysis is used to study the interactions between Castalin, PLGA, physical mixture and the drug loaded nanoparticles and the specturm obtained is presented

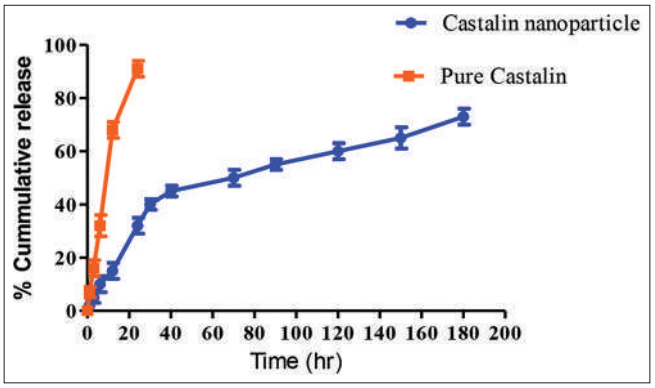

Figure 13: Cumulative percentage drug release of pure drug castalin and castalin nanoparticles in PBS (pH 7.4)

release. Due to the burst effect, the drug from the solution was released fast and finished in 24 h. It was found that there was an initial burst release according to the accumulative release rate of castalin from the NPs, and this result may be due to castalin adhered on the surface of the NPs. A sustained castalin release to about 70 % was possessed for the NPs over 180 h. Thus, the polymer PLGA prevents the castalin burst release and controls the release rate of castalin. In addition, *in vitro* release curve suggests that castalin NPs possessed a remarkable time prolongation effect on castalin release and supports long time stability.

NO Scavenging Assay

The results [Table 5 and Figure 14] of NO scavenging activity of the standard drug cisplatin, castalin, and castalin NPs were shown as percentage of NO or reactive nitrogen species, formed during their reaction with oxygen or with superoxides, such as N02, N2O4, N3O4, NO3-, and NO2 found to be very reactive. These ionic compounds are responsible for altering the structural and functional behavior of many cellular components. The sodium nitroprusside solution is incubated in phosphate buffer saline at 25°C for 2 h resulted in linear time-dependent nitrite production, which was reduced by the tested castalin and castalin NPs. This may be due to the antioxidant principles in the castalin, which compete with oxygen to react with NO, thereby inhibiting the generation of nitrite. Castalin and castalin NPs show approximately equal when compare with standard cisplatin. The maximum NO inhibition percentage of standard cisplatin and castalin and castalin NPs was found to be 92.98%, 67.86%, and 78.22, respectively. IC_{50} values of standard cisplatin and castalin and castalin NPs were found to be 25.66, 22.66, and 23.88, respectively.

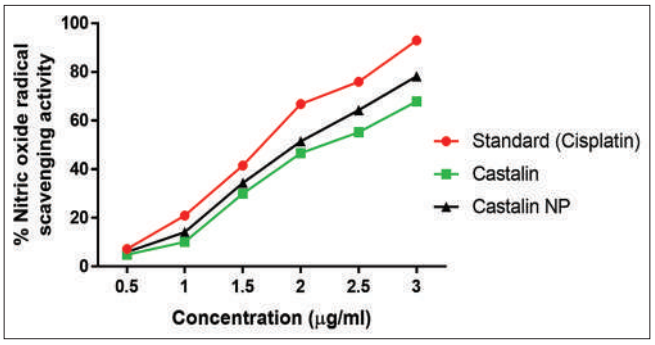

Figure 14: Nitric oxide scavenging assay of standard drug cisplatin, castalin, and castalin nanoparticles

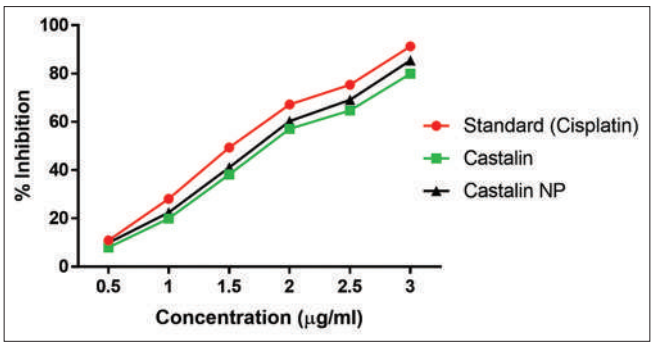

Figure 15: Cytotoxic study of castalin and castalin nanoparticles

Table 5: The results of NO scavenging activity of the standard drug cisplatin, Castalin and Castalin nanoparticles were shown as percentage of Nitric oxide or reactive nitrogen species, formed during their reaction with oxygen or with superoxides

Drug	Concentration (µg/ml)	Absorbance 546 nm	% inhibition	IC_{50}
Control	0.0	0.5301	0.0	25.66
Standard (Cisplatin)	5	0.4892	7.22	
	10	0.4268	20.92	
	20	0.3078	41.56	
	40	0.1576	66.82	
	80	0.1148	75.94	
	160	0.0260	92.98	
Castalin	5	0.5132	4.88	22.26
	10	0.4802	10.12	
	20	0.3622	29.98	
	40	0.2798	46.59	
	80	0.2382	55.18	
	160	0.2104	67.86	
Castalin NP	5	0.4994	5.98	23.88
	10	0.4522	14.12	
	20	0.3368	34.34	
	40	0.2128	51.42	
	80	0.1726	64.26	
	160	0.1098	78.22	

NP: Nanoparticle

Table 6: Castalin and Castalin nanoparticles showed significant dose-dependent inhibition of growth of HepG2 cells at IC50 values

Drug	Concentration (µg/ml)	OD at 590 nm	% inhibition	IC_{50}
Control		0.8156	0.00	46.12
Standard (cisplatin)	10	0.7012	10.89	
	20	0.6102	28.12	
	40	0.4789	49.34	
	80	0.2846	67.24	
	160	0.2159	75.36	
	320	0.1196	91.26	
Castalin	10	0.7580	7.98	42.24
	20	0.6623	19.92	
	40	0.5190	38.23	
	80	0.3265	57.12	
	160	0.2684	64.68	
	320	0.1524	79.98	
Castalin NP	10	0.7336	9.89	44.38
	20	0.6324	22.46	
	40	0.4912	41.12	
	80	0.3068	60.29	
	160	0.2348	69.12	
	320	0.1322	85.48	

NP: Nanoparticle

Cytotoxicity Studies using HepG2 Cell Line by MTT Assay

Castalin and castalin NPs showed significant dose-dependent inhibition of growth of HepG2 cells at IC50 values of 115.2 µg/ml [Table 6 and Figure 15]. It was found that there were cytotoxic effects with increasing concentration on HepG2 cell line from 10 µg to 320 µg concentration. Compared to the untreated Hep G2 cells, only 20% growth and cell proliferation are maintained even in the treated cells.

DISCUSSION

Numerous investigations have been conducted at developing more efficient systems for drug delivery. The most important challenge in the successful formulation of polymeric drug delivery systems involves preparing carrier systems which are capable of encapsulating the desired drug within its structure and then deliver the drug to the cancerous tissues in its active form. The formulation of synthesizing drug-loaded polymeric NPs involves preparation and characterization of drug encapsulated NPs. The fate of a drug after administration *in vivo* depends primarily on the physicochemical properties of the drug and on its chemical structure (21), therefore, physicochemical characterization of drug-loaded NPs system becomes essential. Particle size is an important parameter as it can directly affect the physical stability, cellular uptake, and biodistribution and drug release from the NPs (21). Our formulation of castalin-loaded PLGA NPs using the s/o/w technique resulted in particles with high castalin encapsulation (~91%) with a size range of 35–100 nm. Other studies have reported different castalin formulations such as micellar aggregates.

CONCLUSION

In this study, castalin-loaded PLGA NPs were prepared using a nanoprecipitation technique. Our studies showed that smooth, spherical PLGA NPs were formed and exhibited high yield and drug EE, with a narrow size range of 35 nm–100 nm and mean particle diameter of 45 nm. The *in vitro* castalin release studies from the NPs showed that castalin was released in a sustained manner over a prolonged period of time. Intracellular uptake and cell viability assays also demonstrated efficient uptake and action of the castalin NPs in prostate cancer cell lines. It is, therefore, concluded that PLGA NPs are capable of delivering castalin over a prolonged period achieving a sustained delivery of castalin, thus making it a potential candidate for cancer therapy.

REFERENCES

1. Neha S, Viness P, Yahya E. Advances in the treatment of Parkinson's disease. Prog Neurobiol 2007;81:29-44.
2. Gupta RB, Kompella UB. Nanoparticle Technology for Drug Delivery. New York: Taylor and Francis Group; 2006. p. 273-4.
3. Gordon EM, Cornelio GH, Lorenzo CC 3rd. First clinical experience using a 'pathotropic' injectable retroviral vector (Rexin-G) as intervention for stage IV pancreatic cancer. Int J Oncol 2004;24:177-85.
4. Rockall AG, Sohaib SA, Harisinghani M. Diagnostic performance of nanoparticle-enhanced magnetic resonance imaging in the diagnosis of lymph node metastases in patients with endometrial and cervical cancer. J Clin Oncol 2005;23:2813-21.
5. Shishodia S, Sethi G, Aggarwal BB. Curcumin: Getting back to the roots. Ann NY Acad Sci 2005;1056:206-17.
6. Maheshwari RK, Singh AK, Gaddipati J, Srimal RC. Multiple biological activities of curcumin: A short review. Life Sci 2006;78:2081-7.
7. Duvoix A, Blasius R, Delhalle S, Schnekenburger M, Morceau F, Henry E, *et al*. Chemopreventive and therapeutic effects of curcumin. Cancer Lett 2005;223:181-90.
8. Aggarwal BB, Kumar A, Bharti AC. Anticancer potential of curcumin: Preclinical and clinical studies. Anticancer Res 2003;23:363-98.
9. Wang Z, Zhang Y, Banerjee S, Li Y, Sarkar FH. Notch-1 down-regulation by curcumin is associated with the inhibition of cell growth and the induction of apoptosis in pancreatic cancer cells. Cancer 2006;106:2503-13.
10. Lev-Ari S, Zinger H, Kazanov D, Yona D, Ben-Yosef R, Starr A, *et al*. Curcumin synergistically potentiates the growth inhibitory and pro-apoptotic effects of celecoxib in pancreatic adenocarcinoma cells. Biomed Pharmacother 2005;59 Suppl 2:S276-80.
11. Aggarwal BB, Shishodia S, Takada Y, Banerjee S, Newman RA, Bueso-Ramos CE, *et al*. Curcumin suppresses the paclitaxel induced nuclear factor-kappaB pathway in breast cancer cells and inhibits lung metastasis of human breast cancer in nude mice. Clin Cancer Res 2005;11:7490-8.

Source of Support: Nil. **Conflicts of Interest:** None declared.